Supporting Information for

Low-Crystallinity Mesoporous NiGaFe Hydroxide Nanosheets on Macroporous Ni Foam for High-Efficiency Oxygen Evolution Electrocatalysis

Shi Feng Zai,‡ An Qi Dong,‡ Jian Li, Zi Wen, Chun Cheng Yang,* Qing Jiang*

Key Laboratory of Automobile Materials (Jilin University), Ministry of Education, and School of Materials Science and Engineering, Jilin University, Changchun 130022, China

* *Corresponding authors. Tel.: +86-431-85095371; Fax: +86-431-85095876; E-mails: ccyang@jlu.edu.cn (C. C. Yang); jiangq@jlu.edu.cn (Q. Jiang).*

† Electronic Supplementary Information (ESI) available. See DOI: 10.1039/x0xx00000x

‡ These authors contributed equally to this work.

Materials and methods

Materials: Nickel nitrate hexahydrate [$Ni(NO_3)_2 \cdot 6H_2O$] was purchased from Sinopharm Chemical Reagent Co., Ltd. Gallium nitrate hydrate [$Ga(NO_3)_3 \cdot xH_2O$], ferric nitrate nonahydrate [$Fe(NO_3)_3 \cdot 9H_2O$] and potassium hydroxide (KOH) were obtained from Shanghai Aladdin Biochemical Technology Co. Ltd. Highly purified N_2 and O_2 were supplied by Changchun Juyang Gas Co. Ltd.

Catalyst Preparation: Before electrodeposition, the Ni foam (NF) support was pre-cleaned with 5 M HCl for 20 min to remove the surface nickel oxides layer, and then rinsed with water and ethanol and dried in a vacuum drying oven for further use. Subsequently, electrodeposition was carried out in a three-electrode system using the above cleaned NF as the working electrode, Ag/AgCl (saturated KCl solution) as the reference electrode and a graphite rod as the counter electrode, respectively. In a typical procedure, NF support was first subjected to an ultrasonic pretreatment for 600 s to ensure the electrolyte permeation, where the electrolyte bath contained 25 mM $Ga(NO_3)_3 \cdot xH_2O$, 22.5 mM $Ni(NO_3)_2 \cdot 6H_2O$ and 2.5 mM $Fe(NO_3)_2 \cdot 9H_2O$. The $Ni_{0.65}Ga_{0.30}Fe_{0.05}$/NF was synthesized through a potentiostatic electrodeposition at -1.0 V *vs*. Ag/AgCl at 5 °C for 500 s. After electrodeposition, the resulting electrode was carefully washed with water and ethanol and dried in a vacuum drying oven, obtaining the $Ni_{0.65}Ga_{0.30}Fe_{0.05}$/NF electrode. In order to investigate the effect of Fe content on OER catalytic activity, three comparative electrodes were prepared by regulating the molar ratios of Ni, Ga, Fe nitrate salts (5:5:0, 4.8:5:0.2, and 4:5:1) using a similar procedure to that described for $Ni_{0.65}Ga_{0.30}Fe_{0.05}$/NF (the corresponding molar ratio is 4.5:5:0.5). Note that these electrodes are labeled herein based on the actual molar ratios determined by inductively coupled plasma-optical emission spectroscopy (ICP-OES). For comparisons, different crystalline-degrees were obtained by the post-annealing

treatment of as-obtained $Ni_{0.65}Ga_{0.30}Fe_{0.05}$/NF at 300 and 500 °C (denoted as T_a = 300 °C and T_a = 500 °C).

Material Characterization: The morphology and structure characterizations were carried out on a field-emission scanning electron microscope (SEM, JSM-6700F, JEOL, 15 kV) and a transmission electron microscope (TEM, JEM-2100F, JEOL, 200 kV). The chemical composition analysis was examined by a JSM-6700F equipped with an energy-dispersive X-ray spectrum (EDS). X-ray diffraction (XRD) patterns were recorded on a D/max2500pc diffractometer using Cu Kα radiation. X-ray photoelectron spectroscopy (XPS) was performed on a Thermo ESCALAB-250 spectrometer with a monochromatic Al-Kα source. Raman spectra were obtained on a micro-Raman spectrometer (Renishaw) with a laser of 532-nm excitation wavelength at 0.2 mW. Fourier transform infrared spectroscopy (FTIR) measurements were performed by using an FTIR spectroscopy (6800-50/NEXUS, Thermo Nicolet, USA). ICP-OES (Jobin-Yvon) was carried out to evaluate the ratios of metal elements. The nitrogen adsorption and desorption measurements were conducted on a Micromeritics ASAP 2020 analyzer to obtain the specific area and pore size distribution.

Electrochemical Measurements: Electrochemical measurements were carried out in oxygen-saturated 1 M KOH electrolyte at room temperature. The electrocatalytic processes were performed in a typical three-electrode system with the as-prepared samples as the working electrode, Ag/AgCl (saturated KCl solution) as the reference electrode, a graphite rod as the counter electrode. To circumvent the possible influence of Fe impurities on catalytic performance, the KOH electrolyte was purified by homemade $Ni(OH)_2$ sediments according to previous work.[1] Electrochemical impedance spectroscopy (EIS) was performed under an initial potential of 1.5 V *vs*. reversible hydrogen electrode (RHE) while sweeping the frequency from 100 kHz to

10 mHz and maintaining an AC amplitude of 10 mV. The polarization curve was performed at a scan rate of 1 mV s^{-1} and the potential was calibrated and converted to a RHE scale by E (*vs*. RHE) = E (*vs*. Ag/AgCl) + 0.197 + 0.059 × pH. Moreover, a gas chromatograph [GC-2014 equipped with a thermal conductivity detector (TCD) and a 5 Å Molecular sieve column] was utilized to determine Faradic efficiencies during the OER processes.

Computational Method: All calculations were performed by spin-polarized DFT in the Dmol3 code of the Materials Studio 2017 software.[2] The generalized gradient approximation with Perdew-Burke-Ernzerhof functional (GGA-PBE)[3] was applied to describe the exchange correlation effects. DFT semicore pseudopotentials core treatment with the basis set of double numerical plus polarization (DNP) was implemented for relativistic effects.[4] The periodic structure was created with a 20 Å vacuum slab to avoid the artificial interaction effect between the slab and their mirror images, and a 1×3×1 Monkhorst-Pack K-point was sampled in the Brillouin zone. Grimme method for DFT-D correction was applied to describe the van der Waals forces.[5] For geometry relaxation, the convergence criteria of energy change, gradient, and the displacement were set to be 1.0×10^{-5} Ha, 1.05×10^{-3} Ha $Å^{-1}$, and 9.4×10^{-3} Å, respectively. The bottom two layers were fixed and considered as a bulk structure. The geometrical configurations and charge density difference plots were illustrated with VESTA software.[6]

The computational hydrogen electrode (CHE) model was used to obtain the free energies.[7] The reference potential was set to be reversible hydrogen electrode (RHE),[8] where the chemical potential of the proton-electron pair was determined by one-half of chemical potential of H_2. In alkaline conditions, the OER process occurs *via* four elementary steps:

$$* + OH^- \rightarrow OH* + e^-: \Delta G_1 \quad (1)$$

$$OH* + OH^- \rightarrow O* + H_2O + e^-: \Delta G_2 \quad (2)$$

$$O* + OH^- \rightarrow OOH* + e^-: \Delta G_3 \quad (3)$$

$$OOH* + OH^- \rightarrow O_2 + H_2O + e^- + *: \Delta G_4 \quad (4)$$

The reaction free energy (ΔG) was determined by the difference between the total energy of products and reactants at each step. As a result, the theoretical overpotential η can be obtained from the Gibbs free energy as follows: $\eta = \max[\Delta G_1, \Delta G_2, \Delta G_3, \Delta G_4]/e - 1.23[V]$.

Supplementary Figures

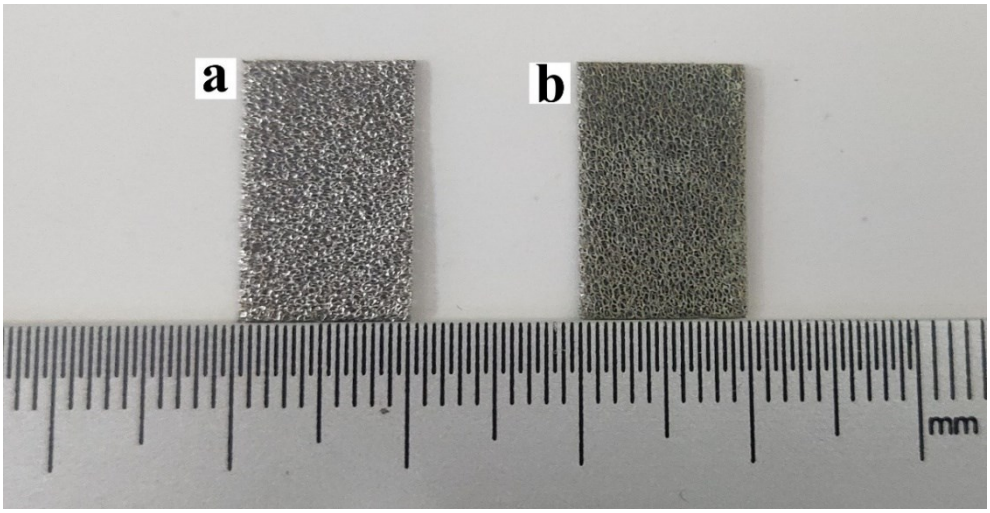

Fig. S1 Photographs of (a) NF support and (b) $Ni_{0.65}Ga_{0.30}Fe_{0.05}$/NF.

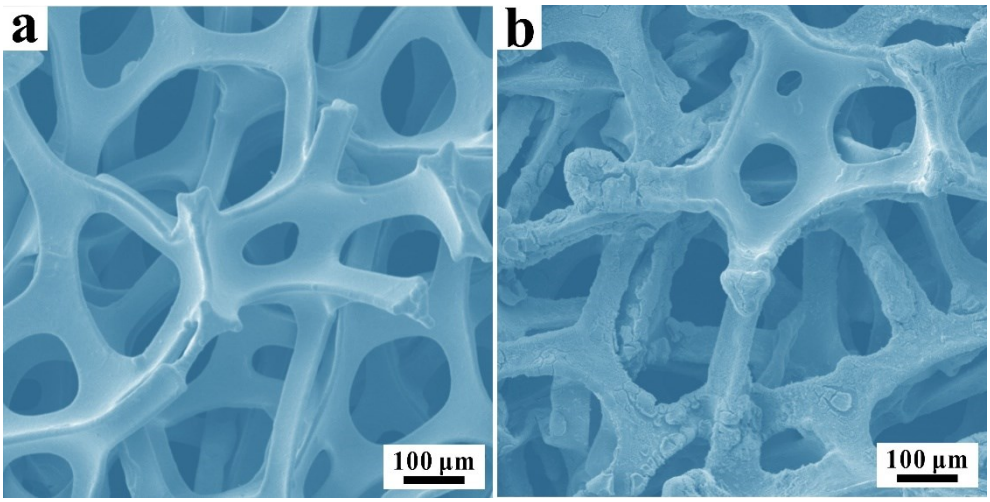

Fig. S2 Low-magnification SEM images of (a) NF support and (b) $Ni_{0.65}Ga_{0.30}Fe_{0.05}$/NF.

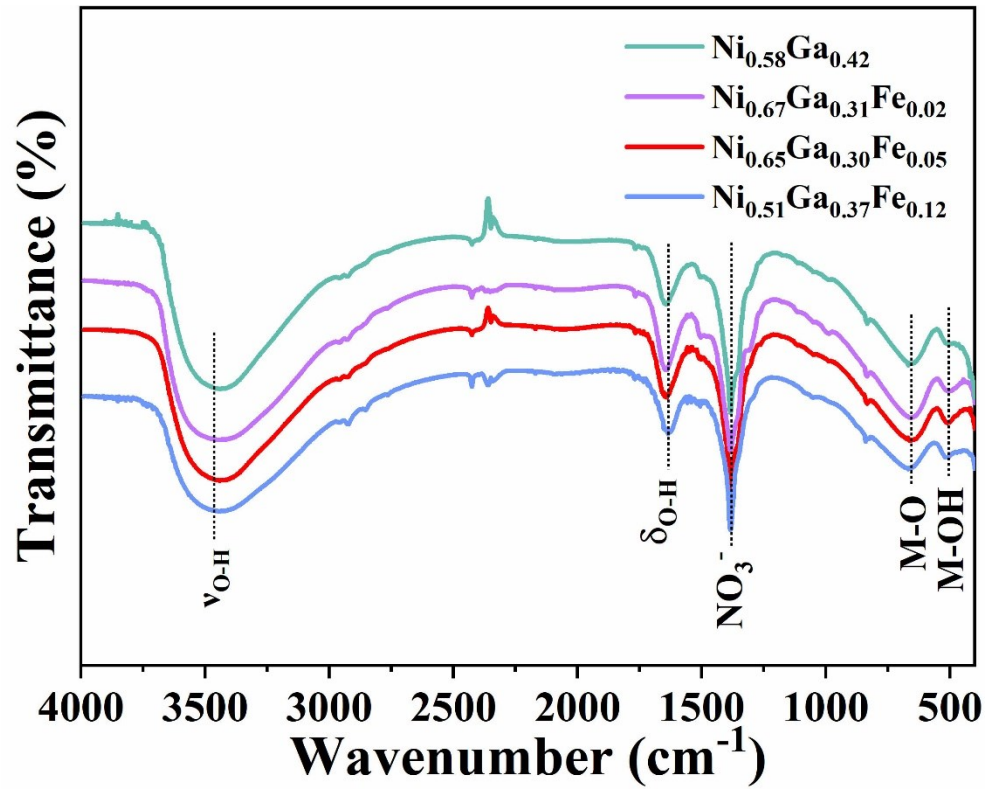

Fig. S3 FTIR spectra of $Ni_{0.58}Ga_{0.42}$, $Ni_{0.67}Ga_{0.31}Fe_{0.02}$, $Ni_{0.65}Ga_{0.30}Fe_{0.05}$ and $Ni_{0.51}Ga_{0.37}Fe_{0.12}$.

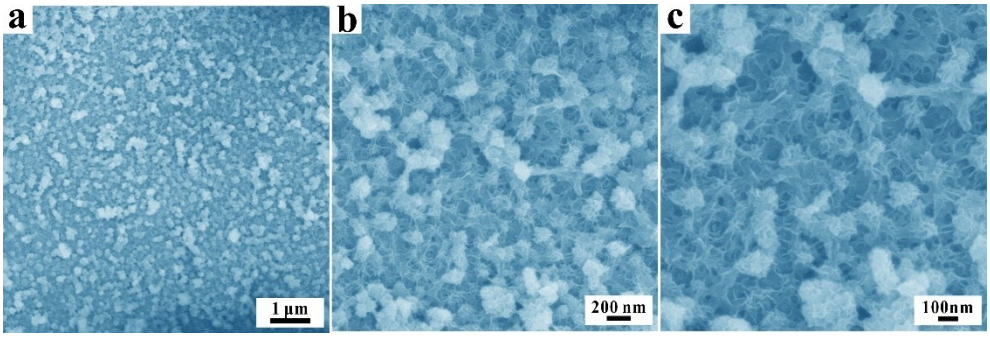

Fig. S4 SEM images of $Ni_{0.65}Ga_{0.30}Fe_{0.05}$/NF.

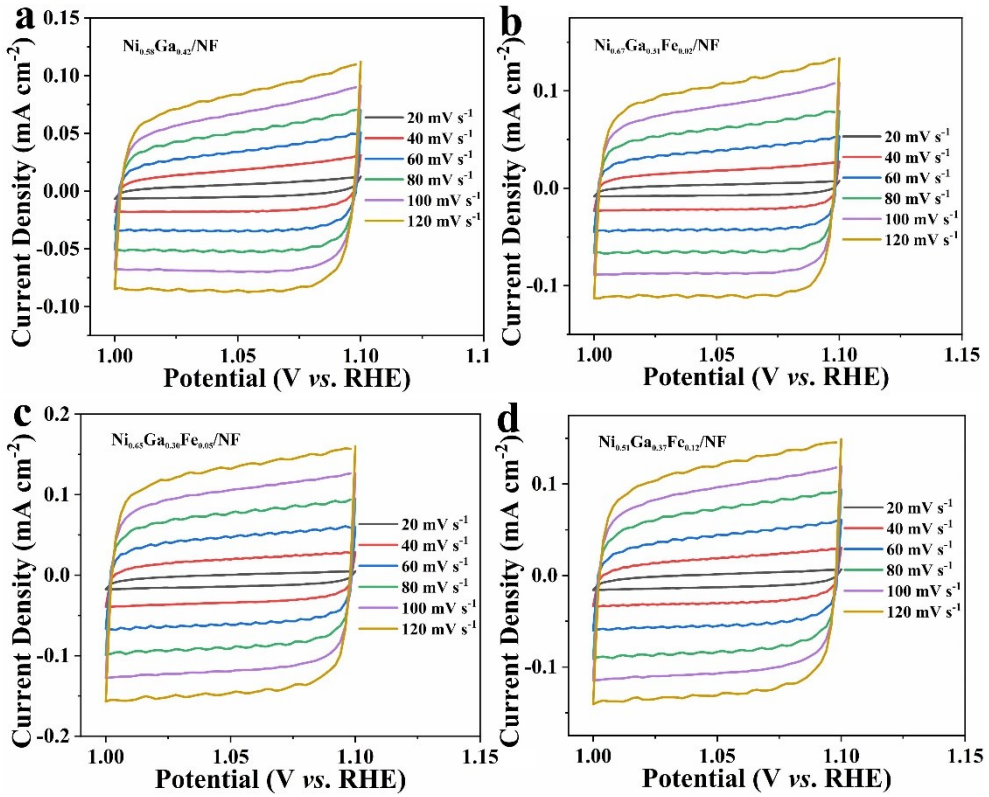

Fig. S5 Cyclic voltammetry curves in the non-Faradaic region at various scan rates for (a) $Ni_{0.58}Ga_{0.42}$/NF, (b) $Ni_{0.67}Ga_{0.31}Fe_{0.02}$/NF, (c) $Ni_{0.65}Ga_{0.30}Fe_{0.05}$/NF and (d) $Ni_{0.51}Ga_{0.37}Fe_{0.12}$/NF.

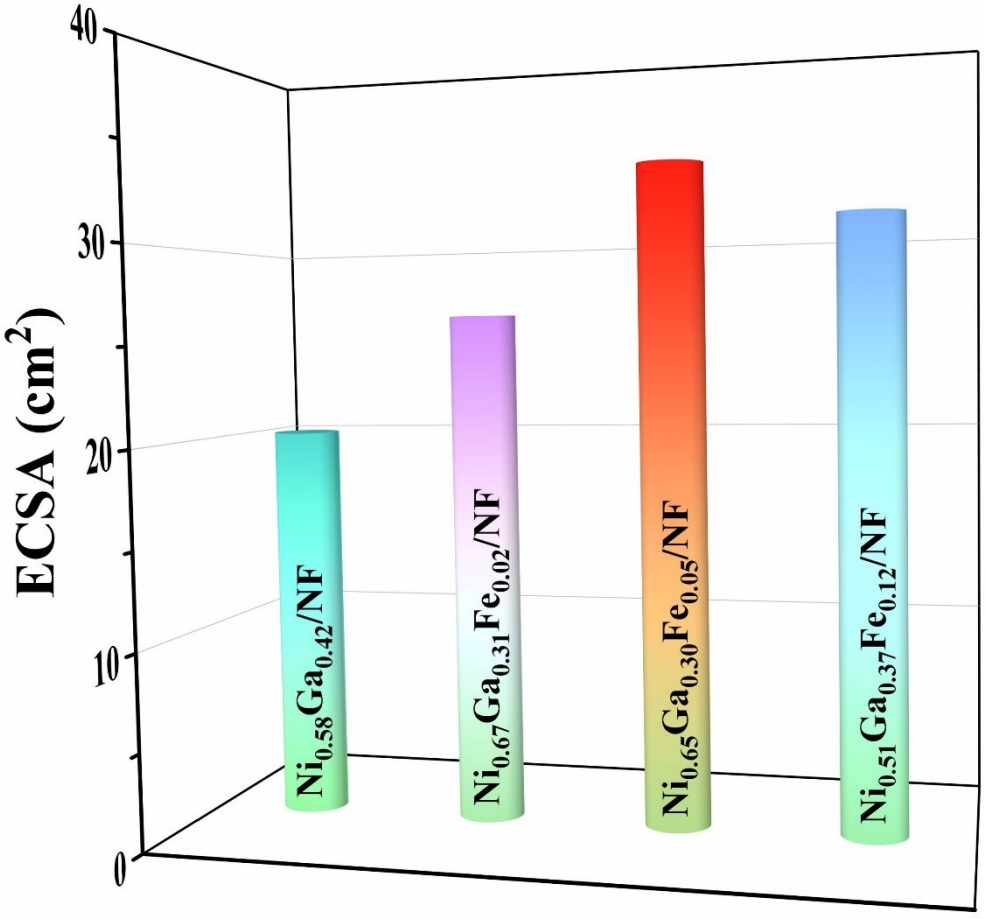

Fig. S6 The calculated ECSA values of $Ni_{0.58}Ga_{0.42}$/NF, $Ni_{0.67}Ga_{0.31}Fe_{0.02}$/NF, $Ni_{0.65}Ga_{0.30}Fe_{0.05}$/NF and $Ni_{0.51}Ga_{0.37}Fe_{0.12}$/NF.

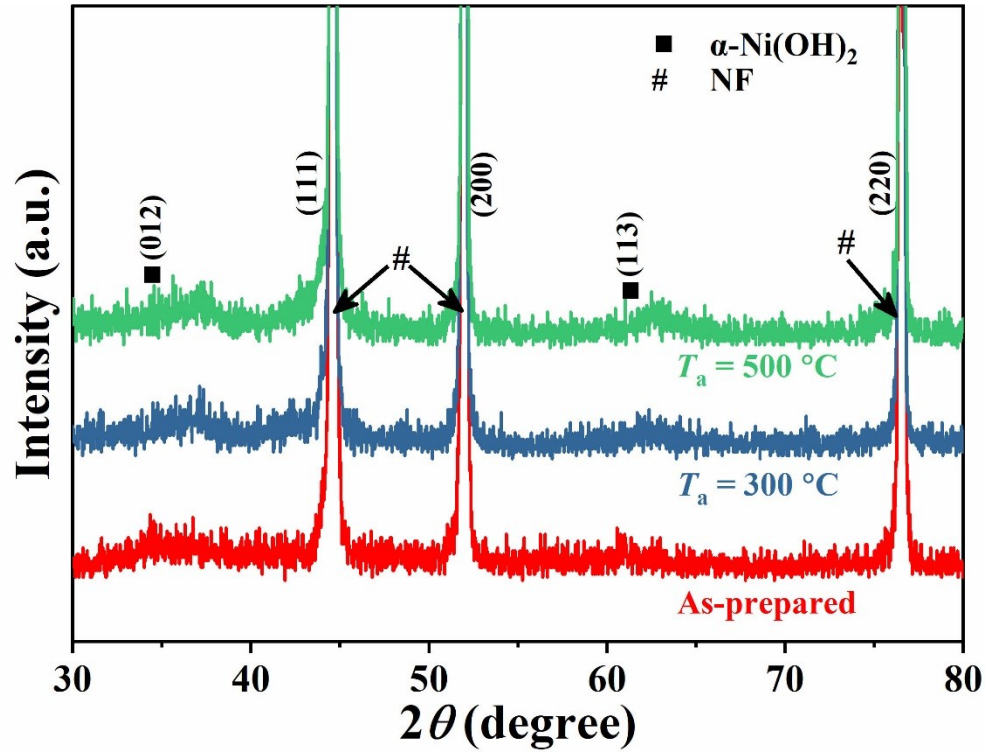

Fig. S7 XRD patterns of as-prepared and annealed (at 300 and 500 °C) $Ni_{0.65}Ga_{0.30}Fe_{0.05}$/NF.

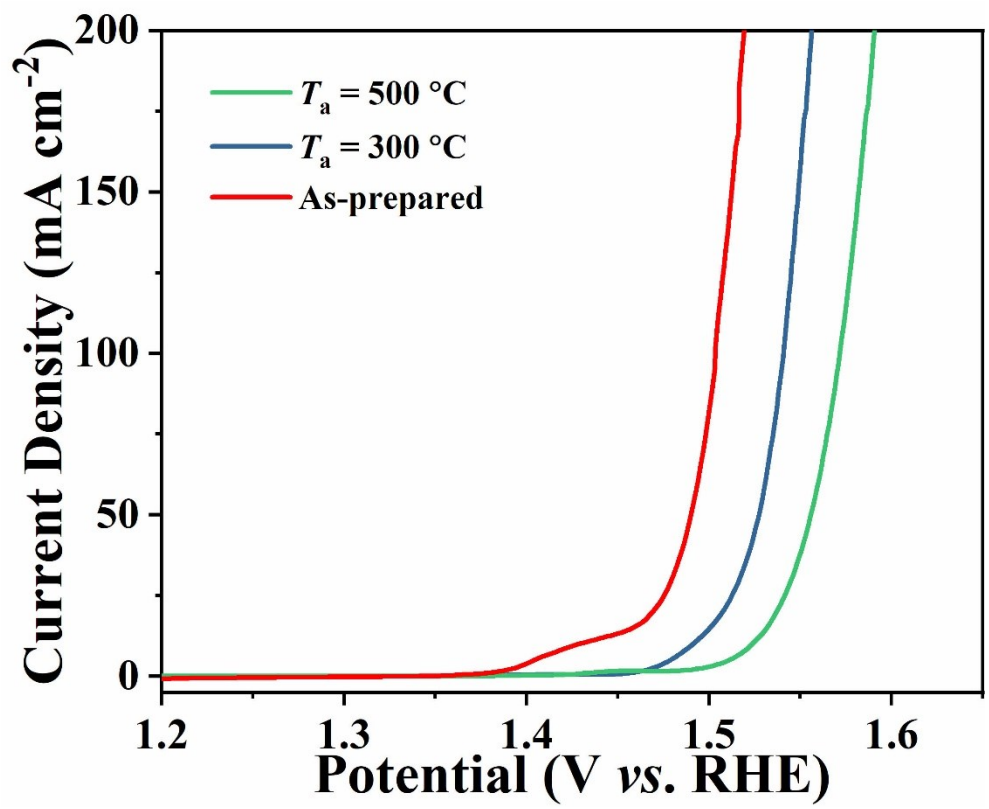

Fig. S8 Polarization curves of as-prepared and annealed (at 300 and 500 °C) $Ni_{0.65}Ga_{0.30}Fe_{0.05}$/NF in 1 M KOH.

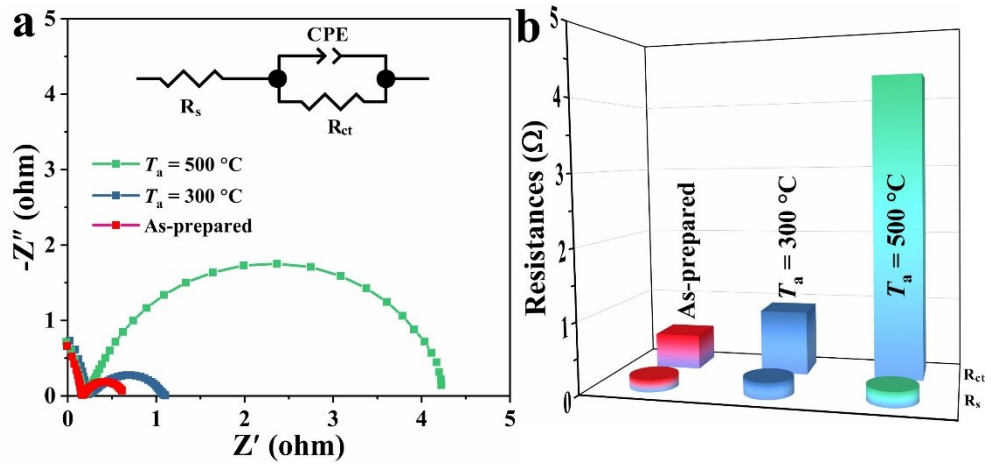

Fig. S9 (a) Nyquist plots of as-prepared and annealed (at 300 and 500 °C) $Ni_{0.65}Ga_{0.30}Fe_{0.05}$/NF. (b) The corresponding charge transfer resistance (R_{ct}) and solution resistance (R_s). The inset in (a) shows an equivalent electrical circuit diagram.

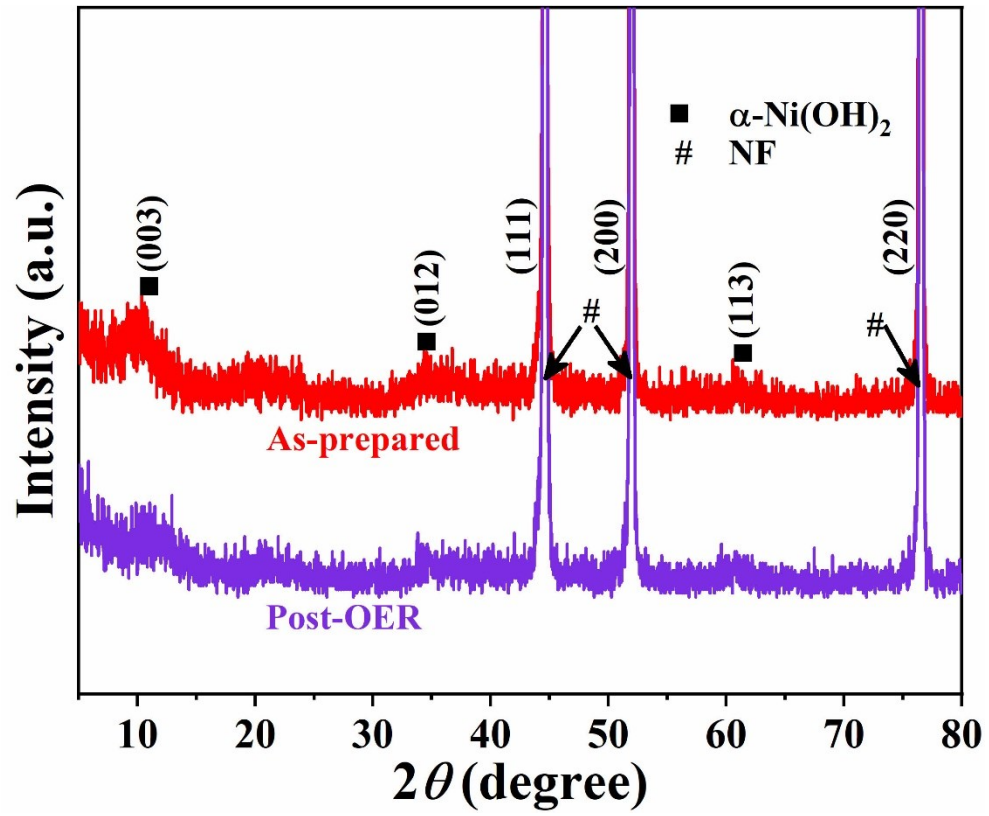

Fig. S10 XRD patterns of the as-prepared and post-OER samples.

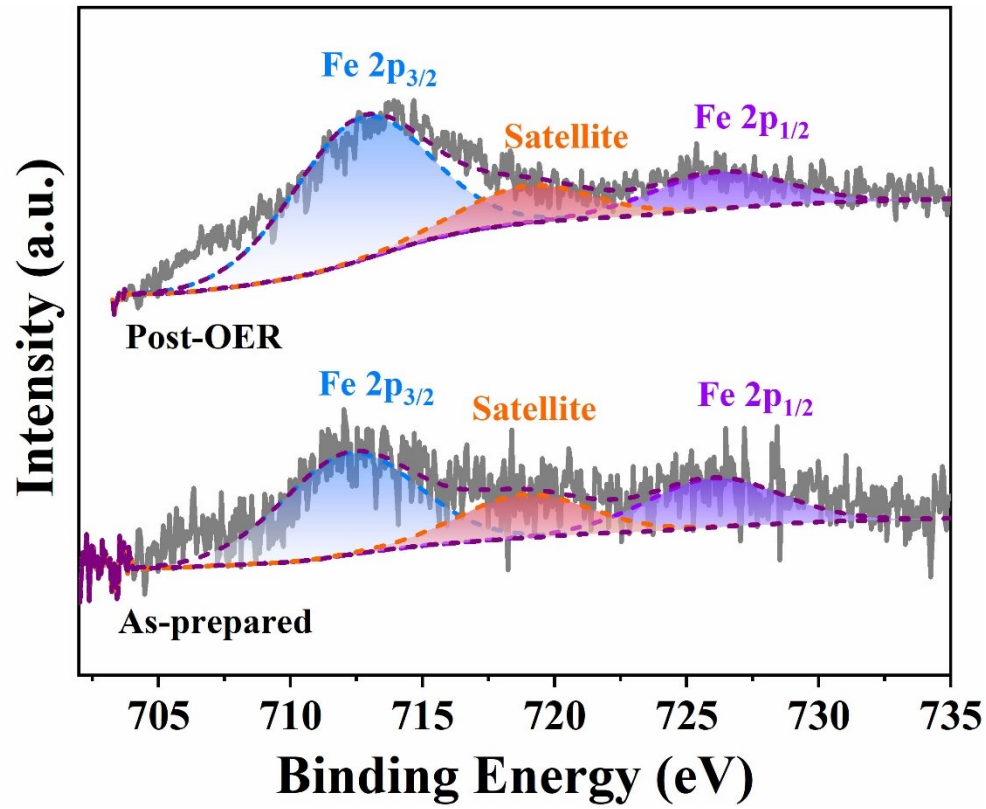

Fig. S11 Fe 2p XPS spectra of the as-prepared and post-OER samples.

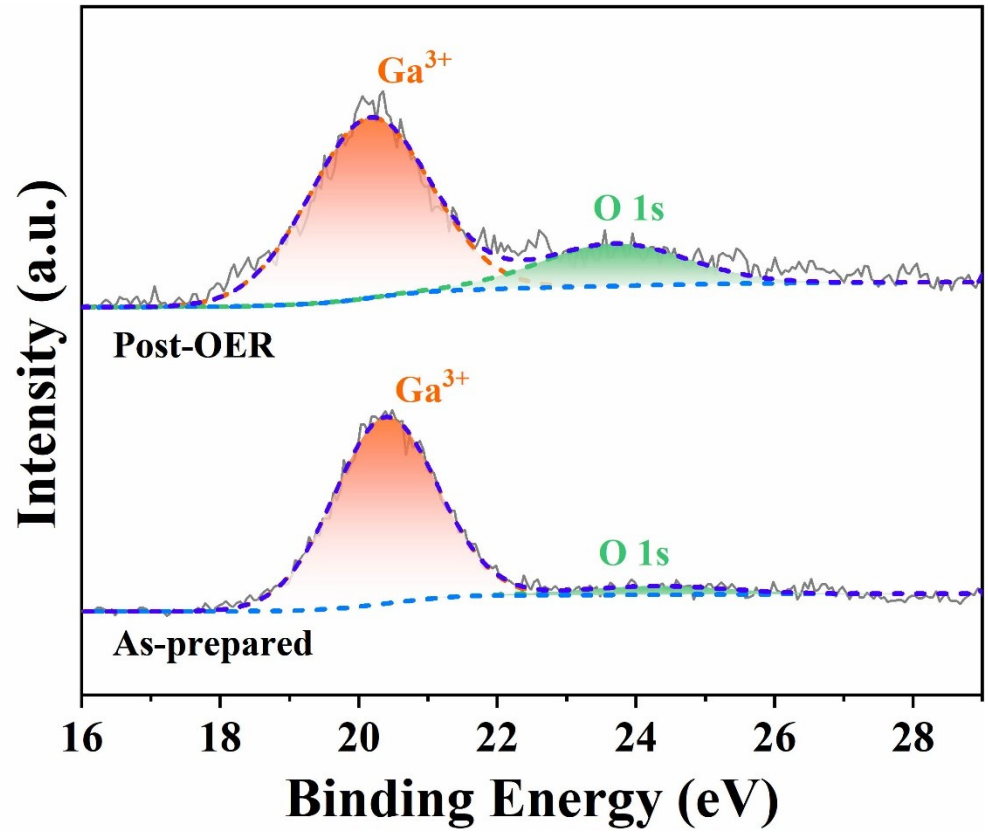

Fig. S12 Ga 3d XPS spectra of the as-prepared and post-OER samples.

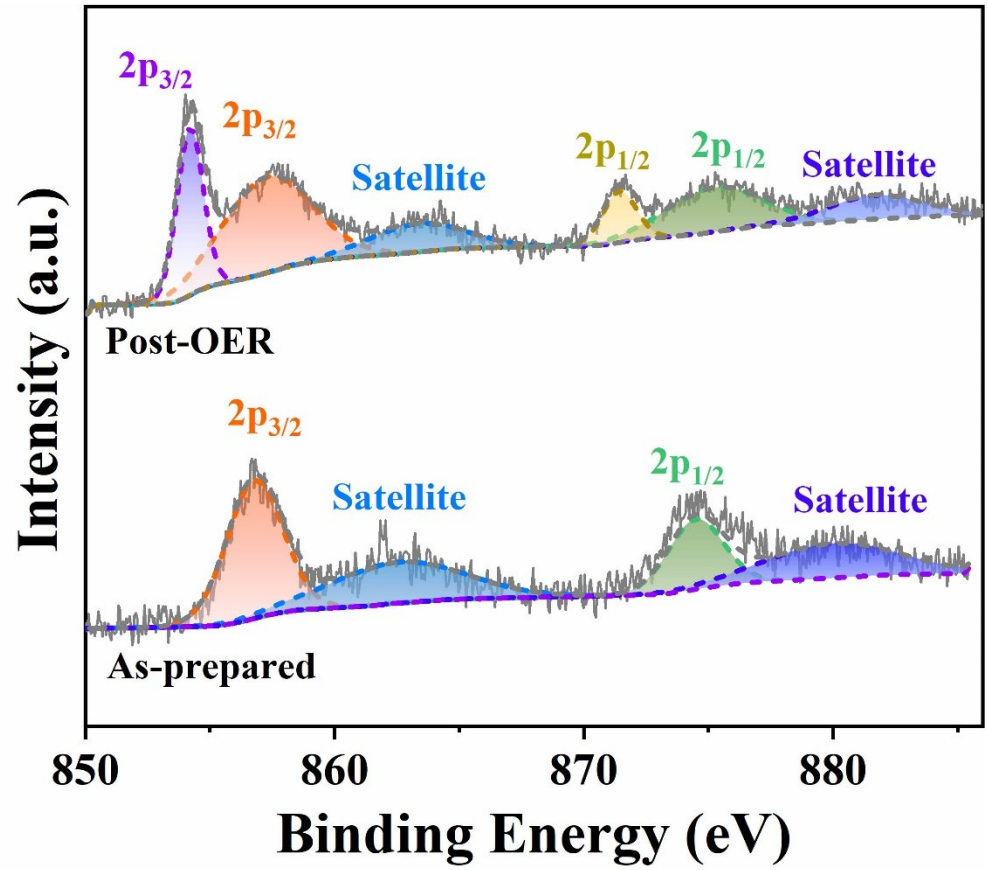

Fig. S13 Ni 2p XPS spectra of the as-prepared and post-OER samples.

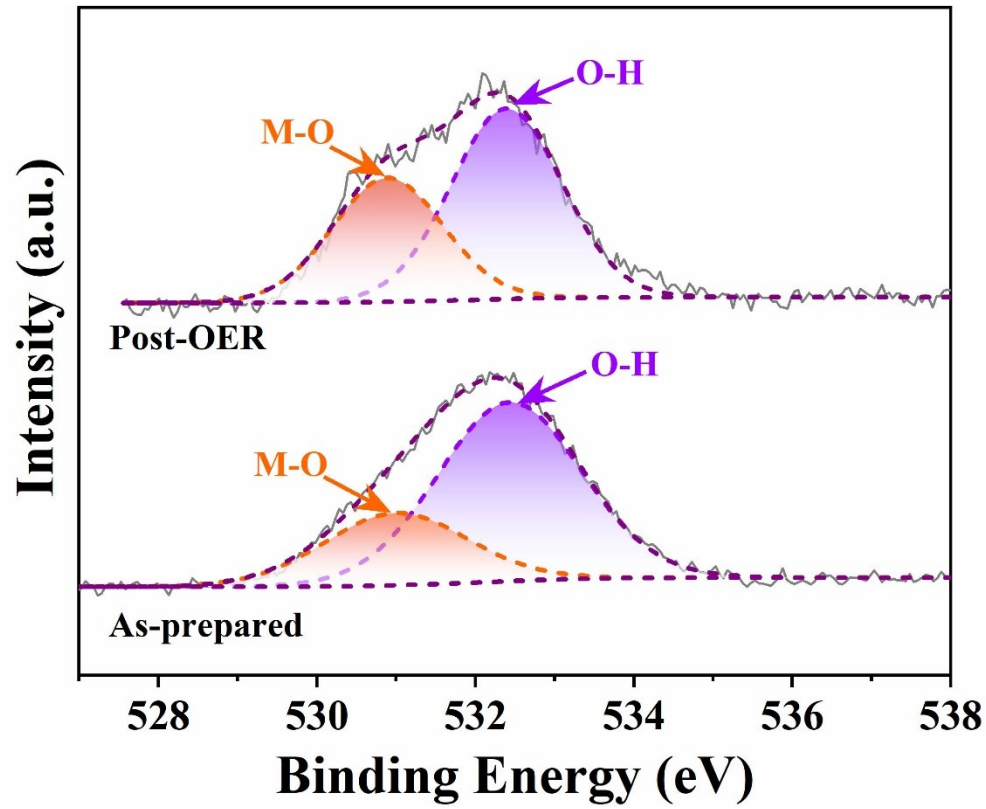

Fig. S14 O1s XPS spectra of the as-prepared and post-OER samples.

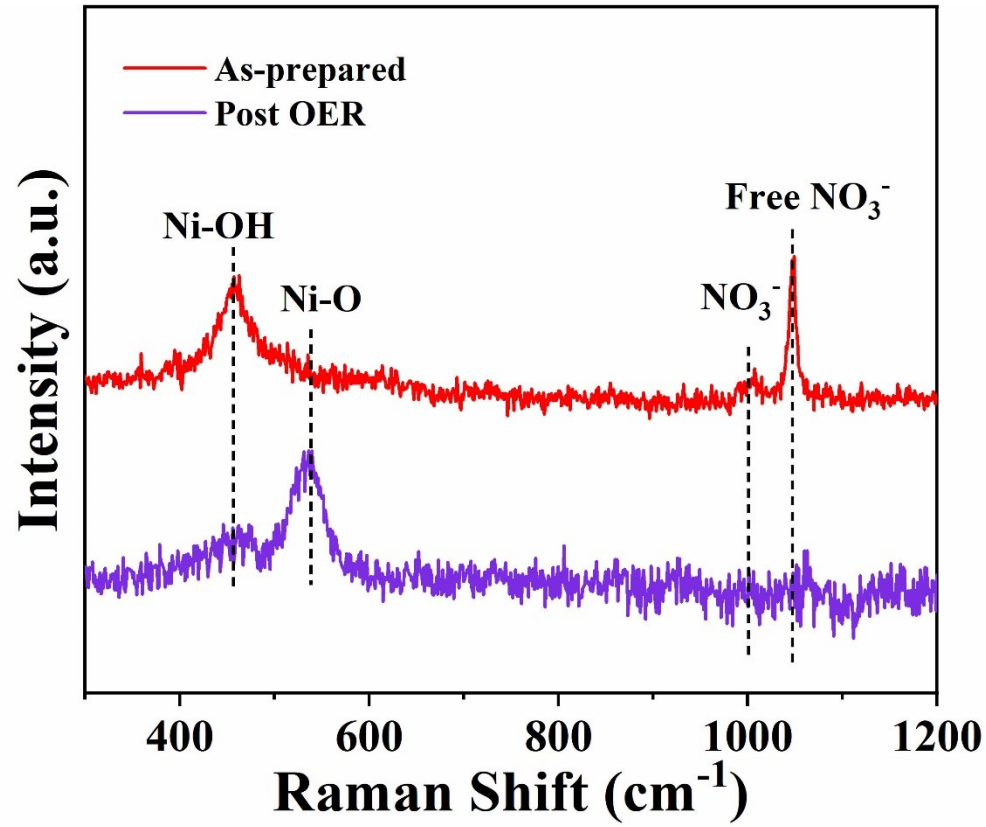

Fig. S15 Raman spectra of the as-prepared and post-OER samples.

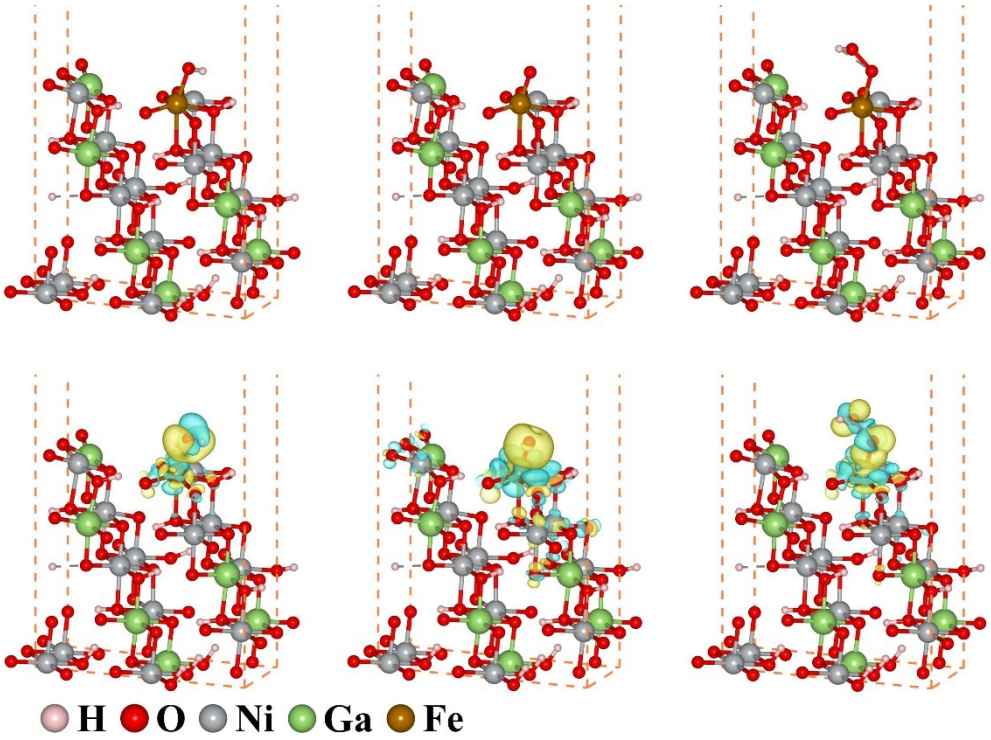

Fig. S16 Differential charge density plots of NiGaFeOOH during the OER process. Yellow and blue areas represent electronic excess and depletion, respectively.

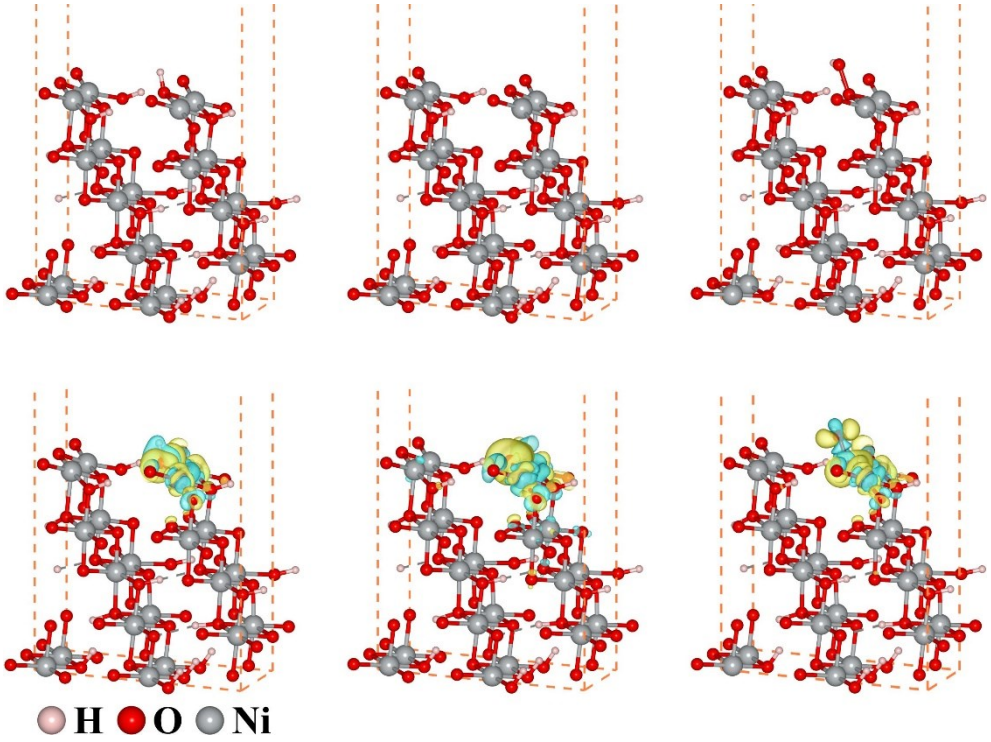

Fig. S17 Differential charge density plots of NiOOH during the OER process. Yellow and blue areas represent electronic excess and depletion, respectively.

Table S1 Comparisons of overpotentials at 10 mA cm^{-2} and Tafel slopes among $Ni_{0.65}Ga_{0.30}Fe_{0.05}$/NF and most of reported OER electrocatalysts in 1 M KOH.

Catalysts	Overpotential (mV) at 10 mA cm^{-2}	Tafel slope (mV dec^{-1})	Ref.
$Ni_{0.65}Ga_{0.30}Fe_{0.05}$/NF	200	42	This work
FeCoW oxy-hydroxides/Au	191	/	Ref.[9] of the text
S-NiCoFe LDH	206	46	Ref.[10] of the text
CoFePi/$Ni(PO_3)_2$/CC	213	39	Ref.[11] of the text
FeNiO/CC	218	47	Ref.[12] of the text
$Co_{0.8}Fe_{0.2}OOH$@C	254	33	Ref.[13] of the text
NiVIr-LDH	180	38	Ref.[14] of the text
NiFeRu-LDH	225	32	Ref.[15] of the text
MoFe:$Ni(OH)_2$/NiOOH	240	47	Ref.[17] of the text
Ni-Fe hydroxides	270	36	Ref.[21] of the text
e-ICLDH@GDY/NF	216	44	Ref.[45] of the text
$W_{0.5}Co_{0.4}Fe_{0.1}$/NF	250	32	Ref.[46] of the text
NiFe/NF	215	28	Ref.[54] of the text
NiCo LDH nanosheets	367	40	[9]
W-$Ni(OH)_2$	237	33	[10]
NiFe-LDH	348	/	[11]
NiV LDH	318	50	[12]
Fe-doped β-$Ni(OH)_2$	219	53	[13]
NiFe-LDHNS@DG10	210	52	[14]
CCS Ni-Co Nw	302	44	[15]
P-FeNiO/CNS	220	52	[16]
Ag@$Co(OH)_x$/CC	250	76	[17]
NiTe/NiS	209	49	[18]
Fe-doped NiO_x nanosheets	310	49	[19]
CoZn(20:1)-P-NS@NF	209	52	[20]
NF@NC-$CoFe_2O_4$/C NRAs	240	45	[21]
$Ni(OH)_2$-NP	260	79	[22]
NiFe LDH@NiCoP/NF	220	49	[23]
Co_3O_4/$Fe_{0.33}Co_{0.66}P$	215	60	[24]
F-CoOOH/NF	270	54	[25]
NiCoON	247	35	[26]
$F_{0.25}C_1CH$/NF	228	42	[27]
$Fe_{17.5\%}$-Ni_3S_2/NF	214	42	[28]
Mn_3N_2	270	101	[29]
Fe/Ni/$Mn_{0.4}$-MIL-53/NF	238	71	[30]
$Co_{1.75}Al_{1.25}O_4$	248	84	[31]
$Fe_3Co_2Al_2$-AE	284	100	[32]
$(Ni_2Co_1)_{0.925}Fe_{0.075}$-MOF	257	41	[33]
Co_3O_4/CeO_2 NHs	270	60	[34]

Fe-Ni_3C-2%	275	62	[35]
YRCO-560	250	34	[36]
NP Au/$CoMoN_x$	237	46	[37]
$NiSe_2$/$CoSe_2$-N	286	53	[38]
V-CoP@a-CeO_2	225	58	[39]
Fe-CoP/CoO	219	52	[40]
$Fe_{0.33}Co_{0.67}OOH$ PNSAs	266	30	[41]
NiCo@$NiCoO_2$/C PMRAs	339	84	[42]
NiFe-UMNs	260	30	[43]
S|NiN_x-PC/EG	280	45	[44]
$Fe_{0.09}Co_{0.13}$-$NiSe_2$	251	63	[45]
NiFeMo	238	35	[46]
CoV-UAH	250	44	[47]
CeO_x/CoO_x	313	66	[48]
$NiNO_{0+15}$	300	74	[49]
CoV_2O_6-V_2O_5/NRGO-1	239	50	[50]
Mn@$Co_xMn_{3-x}O_4$	246	46	[51]
EO Co_3Mo/Cu	220	82	[52]
fcc-NiFe@NC	226	41	[53]
N-CoFe LDHs/NF	233	40	[54]
mesoporous $Ni_{0.8}Fe_{0.2}$ film	206	64	[55]
FeNi-LDH/Ti_3C_2-MXene	298	43	[56]
CoOOH-NS	253	87	[57]
Ni-Fe LDH HNPs	280	49	[58]
CoGa LDH	258	34	[59]
CoFe LDH nanosheets	232	36	[60]

Notes and references

1 J.-S. Sun, Y.-T. Zhou, R.-Q. Yao, H. Shi, Z. Wen, X.-Y. Lang, Q. Jiang, *J. Mater. Chem. A*, 2019, **7**, 9690-9697.

2 B. Delley, *J. Chem. Phys.*, 2000, **113**, 7756-7764.

3 J. P. Perdew, K. Burke, M. Ernzerhof, *Phys. Rev. Lett.*, 1996, **77**, 3865.

4 B. Delley, *Phys. Rev. B*, 2002, **66**, 155125.

5 S. Grimme, *J. Comput. Chem.*, 2006, **27**, 1787-1799.

6 F. L. Hirshfeld, *Theor. Chim. Acta*, 1977, **44**, 129-138.

7 J. K. Nørskov, T. Bligaard, A. Logadottir, J. Kitchin, J. G. Chen, S. Pandelov, U. Stimming, *J. Electrochem. Soc.*, 2005, **152**, J23.

8 J. H. Montoya, C. Tsai, A. Vojvodic, J. K. Norskov, *ChemSusChem*, 2015, **8**, 2180-2186.

9 H. Liang, F. Meng, M. Caban-Acevedo, L. Li, A. Forticaux, L. Xiu, Z. Wang, S. Jin, *Nano Lett.*, 2015, **15**, 1421-1427.

10 J. Yan, L. Kong, Y. Ji, J. White, Y. Li, J. Zhang, P. An, S. Liu, S. T. Lee, T. Ma, *Nat. Commun.*, 2019, **10**, 2149.

11 F. Dionigi, Z. Zeng, I. Sinev, T. Merzdorf, S. Deshpande, M. B. Lopez, S. Kunze, I. Zegkinoglou, H. Sarodnik, D. Fan, A. Bergmann, J. Drnec, J. F. Araujo, M. Gliech, D. Teschner, J. Zhu, W. X. Li, J. Greeley, B. R. Cuenya, P. Strasser, *Nat. Commun.*, 2020, **11**, 2522.

12 K. Fan, H. Chen, Y. Ji, H. Huang, P. M. Claesson, Q. Daniel, B. Philippe, H. Rensmo, F. Li, Y. Luo, L. Sun, *Nat. Commun.*, 2016, **7**, 11981.

13 T. Kou, S. Wang, J. L. Hauser, M. Chen, S. R. J. Oliver, Y. Ye, J. Guo, Y. Li, *ACS*

Energy Lett., 2019, **4**, 622-628.

14 Y. Jia, L. Zhang, G. Gao, H. Chen, B. Wang, J. Zhou, M. T. Soo, M. Hong, X. Yan, G. Qian, J. Zou, A. Du, X. Yao, *Adv. Mater.*, 2017, **29**, 1700017.

15 S.-H. Bae, J.-E. Kim, H. Randriamahazaka, S.-Y. Moon, J.-Y. Park, I.-K. Oh, *Adv. Energy Mater.*, 2017, **7**, 1601492.

16 Z. Liu, B. Tang, X. Gu, H. Liu, L. Feng, *Chem. Eng. J.*, 2020, **395**, 125170.

17 Z. Zhang, X. Li, C. Zhong, N. Zhao, Y. Deng, X. Han, W. Hu, *Angew. Chem. Int. Ed.*, 2020, **59**, 7245-7250.

18 Z. Xue, X. Li, Q. Liu, M. Cai, K. Liu, M. Liu, Z. Ke, X. Liu, G. Li, *Adv. Mater.*, 2019, **31**, e1900430.

19 G. Wu, W. Chen, X. Zheng, D. He, Y. Luo, X. Wang, J. Yang, Y. Wu, W. Yan, Z. Zhuang, X. Hong, Y. Li, *Nano Energy*, 2017, **38**, 167-174.

20 X. Xiao, C.-T. He, S. Zhao, J. Li, W. Lin, Z. Yuan, Q. Zhang, S. Wang, L. Dai, D. Yu, *Energy Environ. Sci.*, 2017, **10**, 893-899.

21 X. F. Lu, L. F. Gu, J. W. Wang, J. X. Wu, P. Q. Liao, G. R. Li, *Adv. Mater.*, 2017, **29**, 1604437.

22 C. Luan, G. Liu, Y. Liu, L. Yu, Y. Wang, Y. Xiao, H. Qiao, X. Dai, X. Zhang, *ACS Nano*, 2018, **12**, 3875-3885.

23 H. J. Zhang, X. P. Li, A. Hahnel, V. Naumann, C. Lin, S. Azimi, S. L. Schweizer, A. W. Maijenburg, R. B. Wehrspohn, *Adv. Funct. Mater.*, 2018, **28**, 1706847.

24 X. Zhang, J. Li, Y. Yang, S. Zhang, H. Zhu, X. Zhu, H. Xing, Y. Zhang, B. Huang, S. Guo, E. Wang, *Adv. Mater.*, 2018, **30**, e1803551.

25 P. Chen, T. Zhou, S. Wang, N. Zhang, Y. Tong, H. Ju, W. Chu, C. Wu, Y. Xie, *Angew. Chem. Int. Ed.*, 2018, **57**, 15471-15475.

26 Y. Li, L. Hu, W. Zheng, X. Peng, M. Liu, P. K. Chu, L. Y. S. Lee, *Nano Energy*, 2018, **52**, 360-368.

27 L. Hui, Y. Xue, D. Jia, H. Yu, C. Zhang, Y. Li, *Adv. Energy Mater.*, 2018, **8**, 1800175.

28 G. Zhang, Y.-S. Feng, W.-T. Lu, D. He, C.-Y. Wang, Y.-K. Li, X.-Y. Wang, F.-F. Cao, *ACS Catal.*, 2018, **8**, 5431-5441.

29 C. Walter, P. W. Menezes, S. Orthmann, J. Schuch, P. Connor, B. Kaiser, M. Lerch, M. Driess, *Angew. Chem. Int. Ed.*, 2018, **57**, 698-702.

30 F. L. Li, Q. Shao, X. Huang, J. P. Lang, *Angew. Chem. Int. Ed.*, 2018, **57**, 1888-1892.

31 X. Wang, P. Sun, H. Lu, K. Tang, Q. Li, C. Wang, Z. Mao, T. Ali, C. Yan, *Small*, 2019, **15**, e1804886.

32 Y. Sun, Y. Xia, L. Kuai, H. Sun, W. Cao, M. Huttula, A. P. Honkanen, M. Viljanen, S. Huotari, B. Geng, *ChemSusChem*, 2019, **12**, 2564-2569.

33 Q. Qian, Y. Li, Y. Liu, L. Yu, G. Zhang, *Adv. Mater.*, 2019, **31**, e1901139.

34 Y. Liu, C. Ma, Q. Zhang, W. Wang, P. Pan, L. Gu, D. Xu, J. Bao, Z. Dai, *Adv. Mater.*, 2019, **31**, e1900062.

35 H. Fan, H. Yu, Y. Zhang, Y. Zheng, Y. Luo, Z. Dai, B. Li, Y. Zong, Q. Yan, *Angew. Chem. Int. Ed.*, 2017, **56**, 12566-12570.

36 M. Kim, B. Lee, H. Ju, S. W. Lee, J. Kim, *Adv. Mater.*, 2019, **31**, e1901977.

37 R. Q. Yao, H. Shi, W. B. Wan, Z. Wen, X. Y. Lang, Q. Jiang, *Adv. Mater.*, 2020, **32**, e1907214.

38 X. Zheng, X. Han, Y. Cao, Y. Zhang, D. Nordlund, J. Wang, S. Chou, H. Liu, L. Li, C. Zhong, Y. Deng, W. Hu, *Adv. Mater.*, 2020, **32**, e2000607.

39 L. Yang, R. Liu, L. Jiao, *Adv. Funct. Mater.*, 2020, **30**, 1909618.

40 X. Hu, S. Zhang, J. Sun, L. Yu, X. Qian, R. Hu, Y. Wang, H. Zhao, J. Zhu, *Nano Energy*, 2019, **56**, 109-117.

41 S. H. Ye, Z. X. Shi, J. X. Feng, Y. X. Tong, G. R. Li, *Angew. Chem. Int. Ed.*, 2018, **57**, 2672-2676.

42 H. Xu, Z. X. Shi, Y. X. Tong, G. R. Li, *Adv. Mater.*, 2018, **30**, e1705442.

43 G. Hai, X. Jia, K. Zhang, X. Liu, Z. Wu, G. Wang, *Nano Energy*, 2018, **44**, 345-352.

44 Y. Hou, M. Qiu, M. G. Kim, P. Liu, G. Nam, T. Zhang, X. Zhuang, B. Yang, J. Cho, M. Chen, C. Yuan, L. Lei, X. Feng, *Nat. Commun.*, 2019, **10**, 1392.

45 Y. Sun, K. Xu, Z. Wei, H. Li, T. Zhang, X. Li, W. Cai, J. Ma, H. J. Fan, Y. Li, *Adv. Mater.*, 2018, **30**, e1802121.

46 F. Qin, Z. Zhao, M. K. Alam, Y. Ni, F. Robles-Hernandez, L. Yu, S. Chen, Z. Ren, Z. Wang, J. Bao, *ACS Energy Lett.*, 2018, **3**, 546-554.

47 J. Z. Liu, Y. F. Ji, J. W. Nai, X. G. Niu, Y. Luo, L. Guo, S. H. Yang, *Energy Environ. Sci.*, 2018, **11**, 1736-1741.

48 J.-H. Kim, K. Shin, K. Kawashima, D. H. Youn, J. Lin, T. E. Hong, Y. Liu, B. R. Wygant, J. Wang, G. Henkelman, C. B. Mullins, *ACS Catal.*, 2018, **8**, 4257-4265.

49 J. Huang, Y. Sun, X. Du, Y. Zhang, C. Wu, C. Yan, Y. Yan, G. Zou, W. Wu, R. Lu, Y. Li, J. Xiong, *Adv. Mater.*, 2018, **30**, e1803367.

50 F.-C. Shen, Y. Wang, Y.-J. Tang, S.-L. Li, Y.-R. Wang, L.-Z. Dong, Y.-F. Li, Y. Xu, Y.-Q. Lan, *ACS Energy Lett.*, 2017, **2**, 1327-1333.

51 C. Hu, L. Zhang, Z. J. Zhao, J. Luo, J. Shi, Z. Huang, J. Gong, *Adv. Mater.*, 2017, **29**, 1701820.

52 H. Shi, Y. T. Zhou, R. Q. Yao, W. B. Wan, X. Ge, W. Zhang, Z. Wen, X. Y. Lang, W. T. Zheng, Q. Jiang, *Nat. Commun.*, 2020, **11**, 2940.

53 C. Wang, H. Yang, Y. Zhang, Q. Wang, *Angew. Chem. Int. Ed.*, 2019, **58**, 6099-6103.

54 Y. Wang, C. Xie, Z. Zhang, D. Liu, R. Chen, S. Wang, *Adv. Funct. Mater.*, 2018, **28**, 1703363.

55 M. Yao, N. Wang, W. Hu, S. Komarneni, *Appl. Catal. B: Environ.*, 2018, **233**, 226-233.

56 M. Yu, S. Zhou, Z. Wang, J. Zhao, J. Qiu, *Nano Energy*, 2018, **44**, 181-190.

57 J. Zhou, Y. Wang, X. Su, S. Gu, R. Liu, Y. Huang, S. Yan, J. Li, S. Zhang, *Energy Environ. Sci.*, 2019, **12**, 739-746.

58 L. Yu, J. F. Yang, B. Y. Guan, Y. Lu, X. W. D. Lou, *Angew. Chem. Int. Ed.*, 2018, **57**, 172-176.

59 J. Zhang, C. Dong, Z. Wang, H. Gao, J. Niu, Z. Peng, Z. Zhang, *Small Methods*, 2018, **3**, 1800286.

60 R. Liu, Y. Wang, D. Liu, Y. Zou, S. Wang, *Adv. Mater.*, 2017, **29**, 1701546.